HIGH QUALITY ELECTRON BEAMS WITH TUNABLE ENERGY PRODUCED BY LASER-PLASMA ACCELERATION

B. Cros†, Ch. Ballage, P. Désesquelles, O. Khomyshyn, M. Masckala, F. Massimo, I. Moulanier, T. L. Steyn, O. Vasilovici, Laboratoire de Physique des Gaz et des Plasmas, CNRS, Université Paris Saclay, Orsay, France
Y.-Yu Chang, F. M. Herrmann[1], A. Irman, M. Laberge, M. Samir, S. Schöbel, U. Schramm[1], P. Ufer[1], Helmholtz-Zentrum Dresden-Rossendorf, Dresden, Germany,
S. Dobosz Dufrénoy, A. Panchal, Laboratoire Interactions, Dynamiques et Lasers, CEA, Université Paris Saclay, Gif-sur-Yvette, France
[1] also at Technische Universität Dresden, Dresden, Germany

Abstract

Laser wakefield acceleration (LWFA) of electrons occurs when an intense short laser pulse focused in an underdense plasma drives in its wake a plasma wave with an amplitude large enough to trap and accelerate electrons. Relativistic electron bunches are easily obtained through this mechanism and have given rise to a large number of studies and publications. Despite these efforts, the achievement of a high quality reliable electron source, ready for use in applications, still needs some developments. Electron beams with high quality, and tunable electron energy, have been achieved by the authors using the DRACO facility (HZDR Dresden), showing that the injection and acceleration processes can be controlled consistently in a gas cell. Dark current free, relativistic electron bunches with energy peaked at tunable values between 60 MeV, and 200 MeV, 40 pC charge in the peak and sub-mrad rms divergence, reaching up to 14pC/MeV/mrad, have been achieved experimentally and reproduced in Particle in Cell (PIC) simulations using measured input parameters. On going work is aimed at increasing the charge in the peak beyond 100pC through new gas cell development.

INTRODUCTION

Laser driven WakeField Acceleration (LWFA) [1] is a concept providing high gradient (> 1 GV/m) electron acceleration through the interaction of intense, short laser pulses with plasmas. In this process, 10 micron-scale plasma cavities, with radial accelerating and focusing fields, are created in the wake of intense laser pulses, providing opportunities for compact accelerator developments. Most of the studies using LWFA include the developments of electron sources, as plasma electrons can be trapped and accelerated in the plasma cavity, generating electron bunches of a few femtosecond (fs) duration at relativistic energy over a few millimeters of plasma.

The so-called mechanism of ionization injection [2] of electrons in a laser driven plasma cavity is a way to create locally a large number of electrons, which can be trapped and accelerated to hundreds of MeVs over millimeter scales. Without additional mechanisms, ionization injection cannot generate high charge density electron beams, and the charge in the beam is proportional to the spatial volume in the plasma over which injection occurs, resulting in energy spectra with large energy spread (100%).

In order to control this process, and achieve electron beams with smaller energy spread, efforts from several groups [3] are aiming at structuring the plasma density profile which contributes to control laser intensity along the propagation and separate the regions of the plasma where electron injection and acceleration take place. In addition, plasma ramps can be used as lenses and dechirpers to further improve beam quality [4].

Coupling laser beams to structured plasmas provides a large number of parameters to tune the electron beam quality and is the main topic of the presented work. Experimental results obtained at the HZDR using the LPGP gas cell are presented and discussed. Analysis of electron dynamics was performed using PIC simulations with the code SMILEI [5].

EXPERIMENT

Experiments were performed at the HZDR centrum using the DRACO laser as a driver for the laser wakefield electron source [6, 7]. A sketch of the experimental set-up is shown in Fig. 1. The laser beam, with a centre wavelength of λ_0 = 0.8 μm, and an energy on target of maximum 3 J, is focused inside the gas cell to a 24 μm FWHM spot size. The duration of each laser pulse is 30 fs FWHM, and a repetition rate of 0.1 Hz is used. The laser distribution in the focal volume is characterized by an almost constant peak intensity on the propagation axis and the transverse distribution is close to a focused flattened gaussian function (order N=8, w_0=14 μm). Measurements of the input laser in vacuum were performed, showing that the laser distribution is characterized by a good symmetry around the propagation axis, with a rotational symmetry parameter [8] larger than 0.8 over a distance of 4 mm in the focal volume. On line diagnostics at focus, and at 2 mm away on each side of the focus were implemented to monitor the transverse and longitudinal focus fluctuations on each shot [9].

† brigitte.cros@universite-paris-saclay.fr

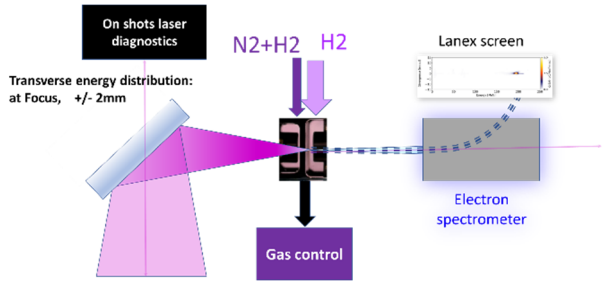

Figure 1: Sketch of experimental set-up illustrating the driver laser geometry and measurement of input parameters through a leaky mirror, the gas cell used to confine and control gas parameters, and the electron spectrometer (magnetic dipole and lanex screen) used for electron energy analysis.

The plasma is created by optical laser-field ionisation of the gas, whose distribution is determined by the geometry of the LPGP gas cell. The gas cell geometry can be changed to study different configurations. A first compartment, C1, of length 0.5 mm along the main axis, contains a mixture of hydrogen gas with a fraction of nitrogen up to 15%. A second compartment, C2, with adjustable length, typically 1.5 mm, is filled with pure hydrogen. Each compartment is ended by faces with small holes to let the gas and laser go through. This creates density ramps with a scale length that can be controlled with the hole diameter (typically 0.5mm). A gap between the two compartments allows to control gas mixing between the two compartments.

Figure 2 illustrates a typical electron density distribution (blue line) achieved inside this 2 compartment gas cell.

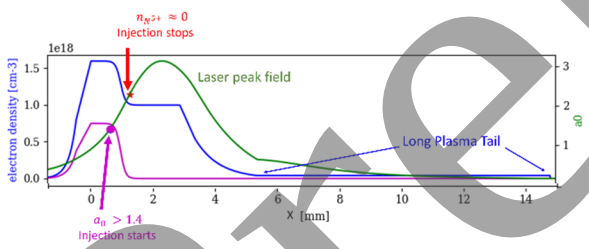

Figure 2: Total electron density (blue line), electron density from ionisation of nitrogen outer shell (purple line) and laser peak normalised electric field (green line, right-hand axis) as functions of position along the propagation axis inside the gas cell; x=0 corresponds to the inner entrance wall of the gas cell.

The gas distribution is calculated from fluid simulations and plateau densities in C1 and C2 are measured off-line by interferometry. The purple line shows the electron density obtained from the ionisation of nitrogen contained in C1. This profile is characterized by a down ramp (3 mm < x < 4.5 mm), followed by a long, low density plasma tail (LPT) which contribute to shape the accelerated electron beam distribution.

Electrons are detected after exiting the gas cell using a dipole magnet and a lanex screen imaged by CCD cameras. The variation of several parameters was studied: laser focus in vacuum with respect to gas cell, density values and shapes.

ELECTRON BEAM CHARACTERISTICS

The laser focus inside the gas cell is set as shown in Fig. 2, in order to release inner shell electrons from nitrogen inside the plasma cavity, which occurs for a value of the normalized peak field a_0 above the ionization threshold of N^{5+}. They are trapped in the plasma cavity and accelerated to relativistic energies over a short distance. Experimentally, these electrons are measured with an energy of around 45 MeV when no gas is injected in C2 (see Fig. 3).

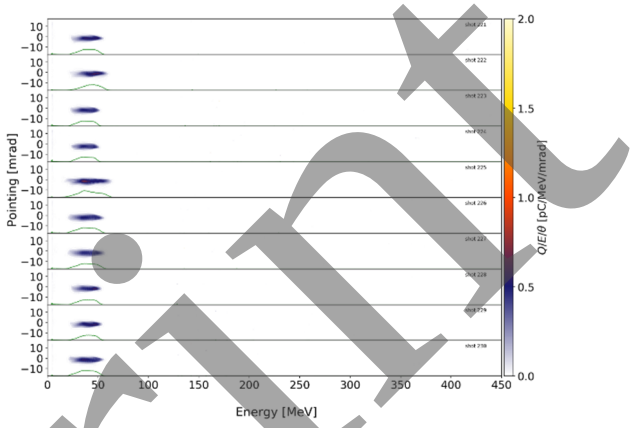

Figure 3: Spectra of electrons generated and pre-accelerated in C1 with 25 mbar, when no hydrogen gas is injected in C2.

When hydrogen gas is added in C2 the electron energy is increased as the plasma length is extended (see Fig. 4).

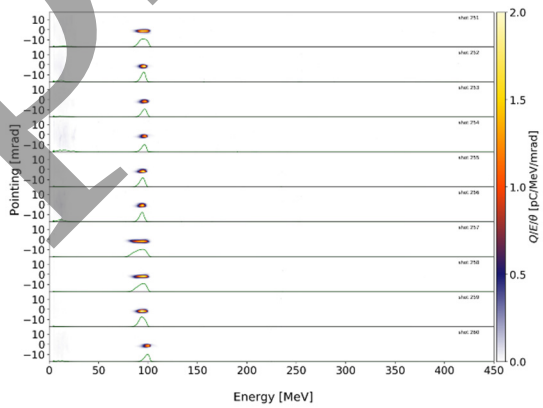

Figure 4: Spectra of electrons accelerated in the same gas cell and conditions as Fig. 3, after injection of 10 mbar of hydrogen in C2.

In addition to increasing the beam energy to 96 +/-2 MeV, the peak height is increased to 4.2 +/-0.5 pC/MeV (FWHM charge 27 +/-10 pC).

The ability to control gas pressure in the two compartments provides a way to tune the electron beam energy as illustrated in Fig. 5. It shows a stack of electron energy spectra measured for the pressure values (P1, P2) in mbar in (C1, C2) indicated in the inserted table. As the pressure is increased, the measured beams have a peak energy continuously tunable, between 79 and 345 MeV in this example, an energy spread between 7 and 3%, and a divergence

between 1 and 0.5 mrad. In addition to pressure, the focus position of the laser beam can be adjusted.

The small divergence, pointing stability, and reduced energy spread are characteristic of the electron beams accelerated in a gas cell. In the examples presented here, they result from the shaping of the electron beam in the down ramp, and the LPT, as shown in simulations [10].

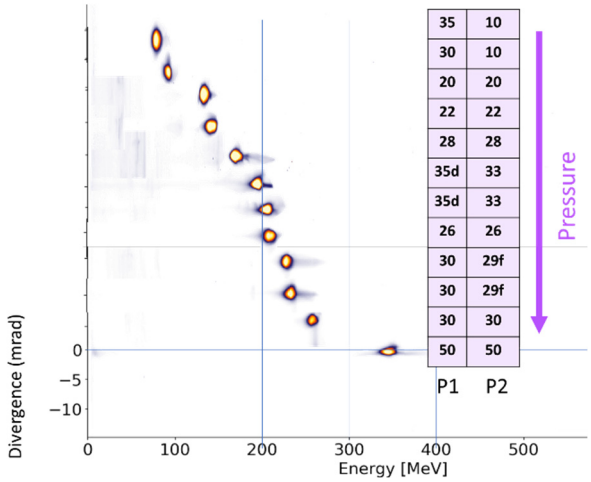

Figure 5: Spectra measured for different gas pressures in C1 and C2 (indicated in the table in mbar) illustrating the possibility of tuning electron beam energy for a fixed gas cell length geometry (C1:0.5mm, gap 1mm, C2:1.5mm).

SIMULATION ANALYSIS

In order to study the dynamics of electron injection and acceleration in this density profile, PIC simulations with the code SMILEI have been performed [4, 10]. Simulations were initiated with a focused flattened gaussian beam model [11] fitting the experimental laser measurements and the density profile obtained from fluid simulations was used [4]. Figure 6 shows an example of electron distribution calculated for 20 mbar.

Spectra of the electron beams in the energy-longitudinal coordinate space are plotted at different positions along the propagation axis to show the evolution of the energy spread. At 3.5 mm (red color spectra), the electron bunch is at the exit of the plateau (see Fig. 2), and entering the down ramp while the laser normalised field is still strong, around 2, and able to drive a plasma cavity with increasing size in the down ramp as the plasma density decreases. At the end of the down ramp (6 mm, blue color), the peak energy has decreased as the front of the bunch has lost energy. In the LPT located between 6 and 15mm, a low-density plasma is created by the laser beam. However, the laser intensity is low and it drives a wakefield with an amplitude negligible compared to the electron beam wakefield. The back of the electron beam is then accelerated in this wake, leading to a spectrum at the end of the LPT with a higher energy and a smaller energy spread, and higher peak height than at the end of the accelerating plateau. The shape of the density profile can thus be used to reduce the chirp of the electron beam and achieve high spectral charge.

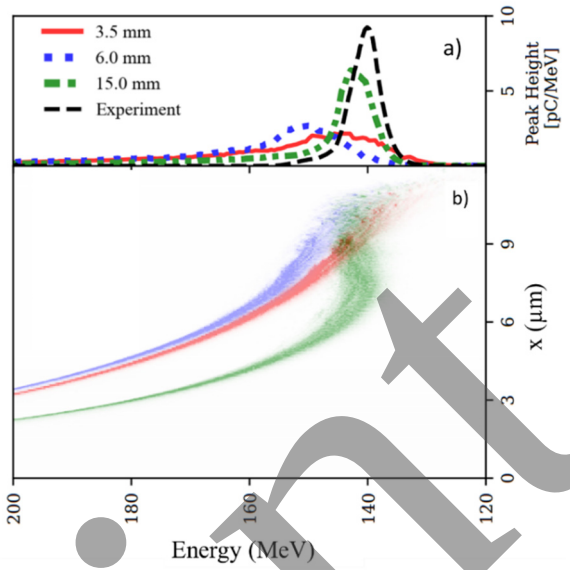

Figure 6: a) Electron spectra calculated in simulations (colour lines) and b) corresponding electron distribution in the space energy-longitudinal position, over a size characteristic of the plasma cavity size. Colours correspond to distributions at different distances of propagation indicated in the legend and corresponding to the beginning of exit down ramp, end of down ramp, and end of LPT (see Fig. 2). The black dashed line is a measured spectrum for a pressure of 20 mbar.

SENSITIVITY TO FLUCTUATIONS

The use of a gas cell provides several assets in favor of electron beam stability:

- Low pressure operation, < 50 mbar, typically 20 mbar giving electron plasma density $n_e = 10^{18}$ cm^{-3};
- Control of gas flow with several parameters allows one to tune finely the density value;
- The shape of gas profile along laser propagation axis is constrained by geometry and reproduceable;
- Tuning gas pressure allows one to tune electron energy for a fixed cell length.

The experimental results presented here have been achieved consistently and reproducibly from day to day, particularly for the energy, pointing and divergence. However, shot-to-shot fluctuations are still large particularly concerning the electron beam charge. This parameter is the most sensitive to laser fluctuations as observed by several groups using different laser systems [12, 13]. In this experiment a strong correlation has been measured between charge fluctuations and +/-100 µm fluctuations of focus position as illustrated in Fig. 7.

The change from negative to positive slope between before and after focus is the signature of a change in focus position as illustrated in the drawing below the graphs. Simulations [10] performed with a change of laser focus of +/- 100 microns with respect to the case illustrated in Fig. 6 confirm this sensitivity.

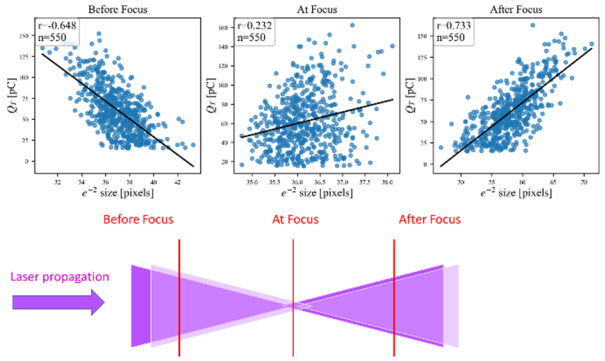

Figure 7: Measured values of total electron beam charge as a function of the corresponding radius of the incident laser beam, measured before, at, and after focus. The drawing illustrates how the measurement of beam size before and after focus is relevant to evaluate the change of focus position. Figure adapted from ref. [10].

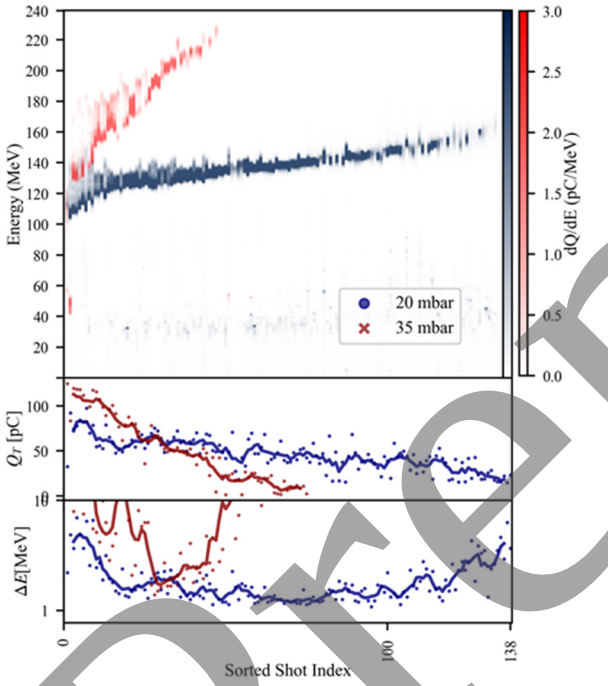

Figure 8: Comparison of measured electron characteristics for 2 different density profile shape at 20 mbar (blue) and 35 mbar (red) for 136 and 30 successive shots, respectively, sorted by increasing energy. From top to bottom, beam energy spectra, total charge, energy spread (Median Absolute Deviation) are plotted as functions of the shot index.

The variation in injected charge leads to large variations in other electron spectra parameters. Examples of electron spectra measured at 20 mbar (blue) and 35 mbar (red) are shown in Fig. 8.

For these data, the nominal parameters were held constant, however laser fluctuations have a strong impact on the charge injected and consequently, on the other properties of the beam. The beams experience beam loading and dechirping in the LPT, that depend strongly on the amount of charge injected. These results show that the use of the LPT for dechirping is optimum in this example for a charge of the order of 40 pC, providing both the highest peak density and the lowest energy spread. In order to minimize the impact of laser fluctuations, different plasma profiles are under study.

CONCLUSION

The reported results show that the control of density profile in gas cell provides high quality electron beams with charge up to 100 pC (10 pC/MeV), energy in the 200 MeV range with 5% spread, a divergence <1 mrad and no dark current. The electron beam energy is tunable by adjusting gas pressure without changing the accelerator geometry. The stability of some parameters (electron beam pointing, beam energy) is improved by using a gas cell operating at low pressure et low non linearity. However, charge fluctuations are still large (25%), and have been shown to be sensitive to fluctuations of laser parameters (wavefront, temporal phase) through the resulting change of longitudinal focus position. Optimisation of density profiles more robust to laser fluctuations will be the topic of future studies.

ACKNOWLEDGEMENTS

This work was granted access to the HPC resources of TGCC and CINES under the allocation 2023-A0170510062 (Virtual Laplace) made by GENCI. The authors acknowledge M. Bisson for the design and management of the MAITRO HPC cluster at LPGP, providing computing resources for data analysis, software development and simulations for the work presented on this paper. This project has received funding from the European Union´s Horizon Europe research and innovation programme under grant agreement no. 101079773 EuPRAXIA, and benefitted from the trans-national access programme under grant agreement no. 871124 Laserlab-Europe, and under grant agreement no. 101131771 Lasers4EU.

REFERENCES

[1] E. Esarey, C. B. Schroeder, and W. P. Leemans, “Physics of laser-driven plasma-based electron accelerators”, *Rev. Mod. Phys.*, vol. 81, no. 3, pp. 1229–1285, Aug. 2009. doi:10.1103/revmodphys.81.1229

[2] M. Chen *et al.*, “Theory of ionization-induced trapping in laser-plasma accelerators”, *Phys. Plasmas*, vol. 19, no. 3, p. 033101, Mar. 2012. doi:10.1063/1.3689922

[3] A. Biagioni *et al.*, “Technical Status Report on Plasma Components and Systems in the context of EuPRAXIA”, Dec. 2024, arXiv:2412.16910 [physics.plasm-ph]. doi:10.48550/arXiv.2412.16910

[4] T. L. Steyn *et al.*, “Simulation of plasma dechirper and lens for laser wakefield acceleration”, presented at IPAC’26, Deauville, France, May 2026, paper TUP3033, this conference.

[5] J. Derouillat *et al.*, “Smilei: A collaborative, open-source, multi-purpose particle-in-cell code for plasma simulation”, *Comput. Phys. Commun.*, vol. 222, pp. 351–373, Jan. 2018. doi:10.1016/j.cpc.2017.09.024

[6] U. Schramm *et al.*, “First results with the novel petawatt laser acceleration facility in Dresden”, *J. Phys. Conf. Ser.*,

vol. 874, p. 012028, 2017.
doi:10.1088/1742-6596/874/1/012028

[7] J. P. Couperus *et al.*, "Demonstration of a beam loaded nanocoulomb-class laser wakefield accelerator", *Nat. Commun.*, vol. 8, Sep. 2017.
doi:10.1038/s41467-017-00592-7

[8] F. Massimo *et al.*, "Laser field reconstruction for the modeling of laser-plasma interaction in cylindrical geometry", *Phys. Rev. E*, to be published.
https://hal.science/hal-05404087v2/document

[9] F. M. Herrmann *et al*., "Tuning of self-truncated ionization injection with bayesian optimization", unpublished manuscript.

[10] T. L. Steyn *et al.*, "Plasma dechirper and lens for electron beams from laser wakefield acceleration in a tailored density profile", Apr. 2026, arXiv:2604.26486 [physics.plasm-ph]. doi:10.48550/arXiv.2604.26486

[11] M. Santarsiero, D. Aiello, R. Borghi, and S. Vicalvi, "Focusing of axially symmetric flattened Gaussian beams", *J. Mod. Opt.*, vol. 44, no. 3, pp. 633–650, 1997.
doi:10.1080/09500349708232927

[12] M. Kirchen *et al*., "Optimal beam loading in a laser-plasma accelerator", *Phys. Rev. Lett*., vol. 126, no. 17, p. 174801, Apr. 2021. doi:10.1103/PhysRevLett.126.174801

[13] S. K. Barber *et al*., "Greater than 1000-fold gain in a free-electron laser driven by a laser-plasma accelerator with high reliability", *Phys. Rev. Lett*., vol. 135, no. 5, p. 055001, Jul. 2025. doi:10.1103/vh62-gz1p